



Short communication

Sensing minute changes in biological cell monolayers with THz differential time-domain spectroscopy

Hai-Bo Liu^a, George Plopper^b, Sarah Earley^b, Yunqing Chen^a,
Bradley Ferguson^{a,c}, X.-C. Zhang^{a,*}

^a Center for Terahertz Research, CII 9009, Rensselaer Polytechnic Institute, Troy, NY 12180, USA

^b Biology Department, Rensselaer Polytechnic Institute, Troy, NY 12180, USA

^c Department of Electrical & Electronic Engineering, The University of Adelaide, SA 5005, Australia

Received 1 December 2005; received in revised form 9 February 2006; accepted 20 February 2006

Abstract

We used terahertz differential time-domain spectroscopy (THz-DTDS) to measure minute changes of bovine lung microvessel endothelial cells (BLMVEC) in response to vascular endothelial growth factor (VEGF). These changes were reflected by alterations in THz wave attenuations and THz dielectric properties of the treated cells. The VEGF-induced THz attenuations of cell monolayers correlated well with changes in transendothelial resistance, as measured using electric cell-substrate impedance sensing (ECIS). However, the morphological differences that gave rise to these changes were not observed with standard optical phase contrast microscopy. We conclude that THz-DTDS is a highly sensitive, non-invasive, powerful new tool to measure minute changes in the morphology of live, cultured cell monolayers. This method enables spectroscopic investigations of cells in the THz band, providing information unavailable through other conventional methods such as optical phase contrast microscopy and ECIS.

© 2006 Elsevier B.V. All rights reserved.

Keywords: THz differential time-domain spectroscopy; Cell monolayer; Cell morphology; Live cell imaging

1. Introduction

Within the past three decades, numerous technologies have been developed for measuring the shape and behavior of individual cells and cell clusters in culture. For example, optical microscopes are the benchmark tools for the characterization of cells in the visible or infrared bands, while electric cell-substrate impedance sensing (ECIS) technology, developed by Applied BioPhysics Inc. (New York, USA), measures the subtle changes in AC impedance (100 Hz–100 kHz) of cell monolayers in real time (Giaever and Keese, 1993). Time-domain dielectric spectroscopy is another well-developed technology used to characterize cell suspensions over a frequency range of 100 kHz–10 GHz (Lisin et al., 1996). What all of these techniques share in common is that they are non-invasive and can be applied to live cells, which allows for

measurements of how these cells respond to specific stimuli over time.

But a wide range of cellular behaviors occur at a small enough scale that they are not detectable using these devices. For example, the electrical impedance across a monolayer of cells is caused by very close association between the plasma membrane of neighboring cells, such that very small changes (on the scale of nanometer distances) can cause dramatic alterations in the paracellular permeability of these monolayers. This is especially true in the microvasculature, where minute changes in endothelial cell shape affect the permeability of capillaries, which in turn affects the transport of nutrients and cellular metabolites through tissues. Devices such as ECIS, which indirectly measure these morphological changes, are not capable of resolving the changes of individual cells within a monolayer. Likewise, even the best optical microscopes cannot resolve structures smaller than 200 nm. Thus, these methods can provide real-time measures of cell behavior, but at the cost of poor resolving power.

A potential solution to this problem is to sense living cells in the THz band (0.1–10 THz), which occupies the portion of elec-

* Corresponding author. Tel.: +1 518 276 3079; fax: +1 518 2763292.
E-mail address: zhangxc@rpi.edu (X.-C. Zhang).

tromagnetic spectrum between the mid-infrared and microwave bands. Biomaterials inside cells, including amino acids, nucleic acids, proteins and DNA have characteristic spectral features in the THz band (Yamaguchi et al., 2003; Fischer et al., 2002; Nagel et al., 2002; Markelz et al., 2002). Historically, the THz band was relatively unexplored as an imaging tool in the biological sciences, due to the absence of powerful sources and efficient detectors. But THz time-domain spectroscopy (THz-TDS), developed in the past decade, now enables us to explore biosensing in the THz band. In THz-TDS, THz pulses are generated and detected by a coherent and time-gated method using near-infrared femtosecond laser pulses. Compared with other THz technologies, THz-TDS holds a much higher signal-to-noise ratio (SNR), ideal for biosensing and identification. Many groups have successfully applied THz-TDS for biomedical study, such as investigating skin tissue and related cancers (Woodward et al., 2002), sensing the far-infrared vibrational modes of DNA components (Fischer et al., 2002), detecting the binding state of DNA (Nagel et al., 2002) and bioaffinity sensing (Mickan et al., 2002; Menikh et al., 2004).

THz differential time-domain spectroscopy improves the SNR of THz-TDS by directly measuring the difference between the THz transmissions of a thin film and its blank substrate. It was originally used to characterize thin dielectric films with sub-micron thickness (Jiang et al., 2000). Due to its high sensitivity and the large absorption coefficient of liquid water in the THz band, THz-DTDS is capable of characterizing very thin water layers. For example, liquid water has an absorption coefficient of $\sim 200 \text{ cm}^{-1}$ at 1 THz at room temperature (Ronne et al., 1997); therefore, the THz amplitude change caused by 1 nm difference of liquid water layer is approximately 10^{-5} . The SNR of the THz-DTDS system can reach 20,000:1, which enables THz-DTDS to sense a 1 nm-thickness difference of liquid water. This is essential to sense live cells, as they consist of more than 70% water (w/w).

Given its potential to resolve small structural details, we decided to apply THz-DTDS to resolve small changes in monolayers of live cells. Specifically, we used vascular endothelial growth factor (VEGF) to induce a flattening and retraction of

endothelial cells within a monolayer, and compared the resolving power of THz-DTDS with conventional phase contrast microscopy and ECIS. Our results demonstrate that THz-DTDS resolves these structural changes with better resolution and precision than either of the more conventional methods.

2. Materials and methods

2.1. Sample preparation

Substrates ($\sim 2 \text{ cm} \times 3 \text{ cm}$) were cut from tissue culture-treated dishes (polystyrene, almost transparent for THz waves). Bovine lung microvessel endothelial cells (BLMVEC) were cultured for 5 days on polystyrene substrates in MCDB 131 complete medium containing antibiotics (VEC Technologies, USA) to 100% confluence at 37°C in a humidified atmosphere containing 5% CO_2 . The growth medium was renewed every other day. The cell confluence was assessed by phase contrast microscopy for the THz-DTDS experiments, and by a plateau in the transendothelial resistance for the ECIS experiments.

Before treatment with VEGF the cells were washed twice with phosphate buffered saline and growth media was changed to a defined medium (Dulbecco's modified Eagle Medium, supplemented with 1%, w/v, bovine serum albumin) without growth factors. VEGF was added to one group of samples at a final concentration of 125 ng/ml in the defined medium. The other group of samples was untreated. Phase contrast images and THz-DTDS measurements were acquired after 3 and 24 h of treatment.

The blank polystyrene substrates were tested with THz-DTDS for their smoothness. The differences between the right half and left half of the blank substrates introduce small THz differential signals at the level of the background noise. Half of the cell monolayer on a substrate was removed to obtain the cell samples for the THz-DTDS measurement, as shown in Fig. 1(a).

Before the THz-DTDS measurements, the cell samples were extracted from the medium and placed in ambient air for about 1 min to dry the cell surface completely. To avoid the possible errors introduced by the incomplete drying, the cell samples were tested by THz transmission measurements before the THz-

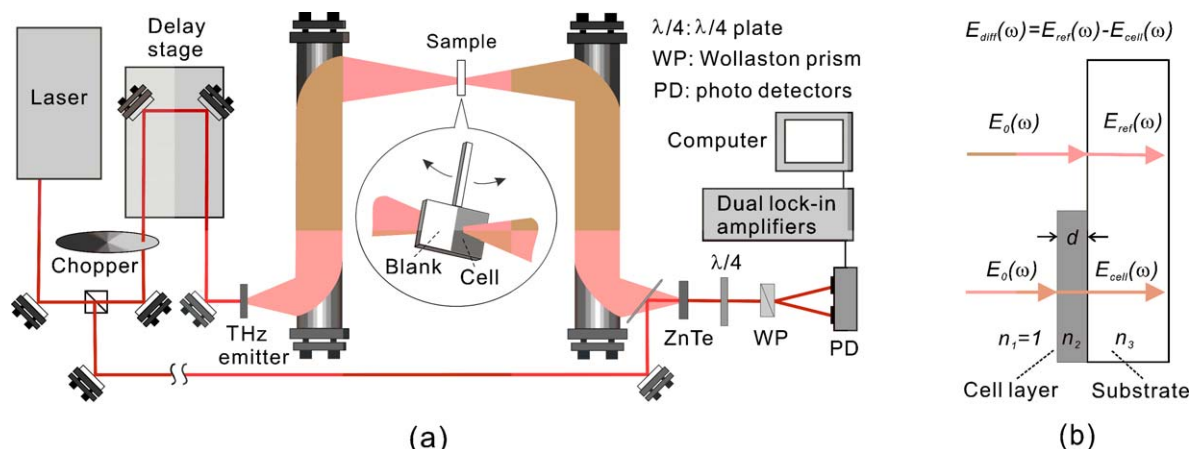


Fig. 1. (a) A schematic diagram of the THz differential time-domain spectroscopy system with an illustration of a cell monolayer sample. (b) A schematic illustration used to determine the differential signal between the reference (blank substrate) and the cell monolayer sample.

DTDS measurements. THz-DTDS measurements were usually made after the samples were dried in ambient air for about 1 min to ensure the surface water was completely evaporated.

2.2. Apparatus and methods

Fig. 1(a) is a schematic of a THz-DTDS system. In this work, the THz emitter was an AC (10 kHz sinusoidal wave) driven GaAs antenna. The pump laser was a Tsunami femtosecond laser (Spectra-Physics, USA), with a pulse duration of ~ 100 fs, wavelength of 800 nm, and average power of 1.3 W. The generated THz pulses propagated through four off-axis parabolic mirrors and were focused on a 2 mm thick (1 1 0) ZnTe crystal, wherein the probe beam detected the THz field via electro-optic sampling (Wu et al., 1996). The sample was placed between the second and third parabolic mirrors, with the THz beam focused on it. A galvanometer-controlled sample holder shook the sample with a frequency of 20 Hz and an amplitude of ~ 5 mm, causing the THz beam to alternately transmit through the cell monolayer (sample) and blank substrate (reference). The system measured the THz transmission difference between the sample and reference. Fig. 1(a) illustrates a schematic of THz-DTDS measuring a cell monolayer sample and Fig. 1(b) shows an illustration used to determine the differential signal between the cell monolayer and the blank substrate (see Section 3.1 for detailed description). Each measurement took approximately 1 min. The THz pulse had a pulse width of ~ 2 ps and a spectral bandwidth of 0.1–2.0 THz. THz-DTDS typically has a SNR five times better than conventional THz-TDS. In addition, THz-DTDS measures the difference between the sample and reference at a modulating frequency, e.g. 20 Hz. This alleviates difficulties associated with temporally varying effects of water vapor absorption in ambient air.

Bright-field images of the BLMVEC samples were obtained using a 10 \times objective Nikon Eclipse TE2000 fluorescence inverted microscope equipped with a digital camera and SPOT image capturing software.

ECIS 1600R (Applied BioPhysics Inc., USA) was used to measure the resistance of BLMVEC monolayers in the vertical direction, the same as the THz transmission direction in THz-

DTDS measurement. ECIS arrays were prepared by adding a gelatin solution to each well (0.5 cm \times 1 cm). The gelatin coats the well bottoms and provides a substrate, which the endothelial cells adhere to. Wells were washed three times using phosphate buffered saline then seeded with BLMVEC. The cells were allowed to grow to confluence for 4 days. The arrays were plugged into the instrument and a baseline measurement of transendothelial resistance was obtained. Approximately, 1 h later, the growth medium was exchanged for a defined medium with and without VEGF. ECIS measurements were taken over a period of approximately 40 h.

3. Results and discussion

3.1. THz-DTDS results

The THz differential waveforms of blank substrate, the untreated cell sample and VEGF-treated cell sample (for 3 h) are shown in Fig. 2(a). All the measurements results obtained at room temperature in ambient air. The THz differential signal peaks of the cell monolayers were higher than that of the acellular (blank) substrates, indicating that we were able to identify the cell monolayers on the substrates with no difficulty. Importantly, the THz differential signal peak of VEGF-treated BLMVEC was 29% lower than that of the matched, untreated cells after only 3 h of VEGF exposure (9.1 versus 6.5 in arbitrary units, with a fluctuation of approximately 0.2). Optical phase contrast microscopy images revealed no noticeable morphological differences between treated and untreated samples, as shown in Fig. 2(b and c), demonstrating that the cellular structural changes accounting for the different THz signals were too subtle to detect by conventional means.

After 1 day of VEGF treatment, the difference between the peak differential signals of the treated and untreated BLMVEC increased to 43% (9.0 versus 5.1), as shown in Fig. 3(a). The 1-day VEGF exposure resulted in a subtle but noticeable change in cell morphology, as shown by the phase contrast images in Fig. 3(b and c). However, phase contrast microscopy lacks the resolving power to detect changes in the principal cellular structure targeted by VEGF: the tight junction (or zonula occludens).

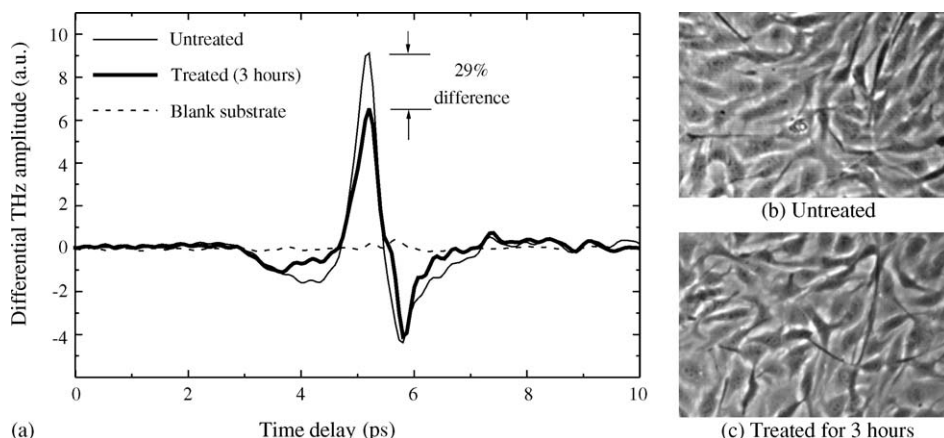


Fig. 2. (a) THz differential waveforms of blank substrate, untreated BLMVEC, and VEGF-treated BLMVEC (for 3 h). (b and c) Optical phase contrast microscopy images of BLMVEC before and after the treatment (for 3 h), respectively.

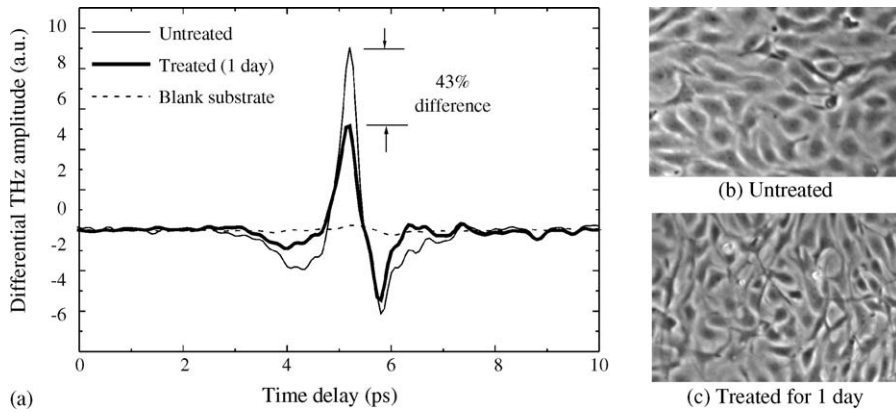


Fig. 3. (a) THz differential waveforms of the blank substrate, untreated BLMVEC and VEGF-treated BLMVEC (for 1 day). (b and c) Optical phase contrast microscopy images of BLMVEC before and after the treatment (for 1 day), respectively.

The tight junction is formed by close apposition of the lateral membranes of adjacent endothelial cells, such that the intercellular spacing between cells is as small as 10–15 nm. The increases in permeability induced by VEGF therefore increase the size of this spacing. But this size is well below the practical threshold of even the best light microscopes (200 nm), so that even relatively large changes in the spacing are not detectable by conventional light microscopy. To directly observe this change in *living* cells is simply impossible using these microscopes.

The decrease of the THz differential signal is most likely due to morphological changes in the cells after the VEGF treatment. A simplified model assumed for the THz wave transmission through a cell monolayer may help elucidate the mechanism of the THz differential signal decrease. Fig. 1(b) illustrates a schematic used to determine the THz differential signal between the reference (blank substrate) and the cell monolayer. In this model, the cell monolayer is represented as a thin film, with a thickness of d and a refractive index of $n_2(\omega)$. ω is the circular frequency, $E_0(\omega)$ the incident field, $E_{\text{ref}}(\omega)$ the reference field and $E_{\text{cell}}(\omega)$ is the transmitted field after cell monolayer. n_1 and n_3 are the refractive indices of the air and the substrate, respectively. r_{ij} and t_{ij} represent the reflection and transmission coefficients of $i \rightarrow j$ interface, respectively ($i, j = 1, 2$ and $3, i \neq j$). According to the Fresnel's Law, the reference field is:

$$E_{\text{ref}}(\omega) = t_{13} \exp\left(\frac{i\omega d}{c}\right) E_0(\omega). \quad (1)$$

By considering the multireflection within the monolayer (Born and Wolf, 1970), the field $E_{\text{cell}}(\omega)$ can be written as:

$$E_{\text{cell}}(\omega) = \frac{t_{12}t_{23} \exp[i\delta(\omega) - \alpha(\omega)d]}{1 - r_{21}r_{23} \exp[2i\delta(\omega) - 2\alpha(\omega)d]} E_0(\omega), \quad (2)$$

where $\alpha(\omega)$ is the amplitude absorption coefficient of the cell monolayer and $\delta(\omega)$ is the phase change of the field after the cell monolayer,

$$\delta(\omega) = \frac{n_2(\omega)\omega d}{c}, \quad (3)$$

where c is the speed of the light in vacuum. For a thin sample, like a cell monolayer with a thickness approximating $1 \mu\text{m}$, $d \ll c/\omega$,

therefore $\delta(\omega) \ll 1$. Under this approximation, we have

$$E_{\text{diff}}(\omega) \approx i \frac{\omega}{c} E_{\text{ref}}(\omega) d \left[n_2 - 1 + \frac{(n_2 - n_1)(n_2 - n_3)}{(n_1 + n_3)} \right] - E_{\text{ref}}(\omega) \alpha(\omega) d \left[1 + \frac{(n_2 - n_1)(n_2 - n_3)}{(n_1 + n_3)} \right], \quad (4)$$

where $E_{\text{diff}}(\omega) = E_{\text{ref}}(\omega) - E_{\text{cell}}(\omega)$. Therefore, $E_{\text{diff}}(\omega)$ is proportional to the thickness of the monolayer sample d and is dependent on the complex THz dielectric property (refractive index $n(\omega)$ and absorption coefficient $\alpha(\omega)$) of the cell monolayers. The THz differential signal differences between the untreated cells and the treated cells for 3 h and those for 1 day are 29 and 43%, respectively. Since a 10–30% thickness change is within a normal range after the treatment for these cells, we assume that the thickness change of the BLMVEC monolayers is a main factor contributing to the THz differential signal differences upon the VEGF treatment. Based upon Eq. (4), the refractive index $n(\omega)$ and absorption coefficient $\alpha(\omega)$ have a relatively smaller effect on the THz differential signal. $n(\omega)$ and $\alpha(\omega)$ were hardly measured using THz-DTDS because the cell monolayers were not uniform films and their exact thickness values were not available. Therefore, we could only give an approximate estimation. Assuming $n(\omega) = 2.2$, $\alpha(\omega) = 200 \text{ cm}^{-1}$ (the same as liquid water) and $d = 2 \mu\text{m}$, a 20% decrease of $n(\omega)$ without a change of $\alpha(\omega)$ will result in $\sim 5\%$ reduction of the THz differential signal. Another contribution was assumed from the increased spacing between cells after VEGF treatment, which enhanced the THz transmission across the cell monolayer and thereby decreased the THz differential signal. While conventional phase contrast light microscopy failed to detect these subtle morphological variations, they were readily detectable with THz-DTDS.

3.2. Comparison between ECIS and THz-DTDS results

As illustrated in Fig. 4(a), we used ECIS to confirm that VEGF induced the characteristic, precipitous drop in transendothelial resistance that accompanies BLMVEC cell flattening and retraction, under the same conditions that yielded

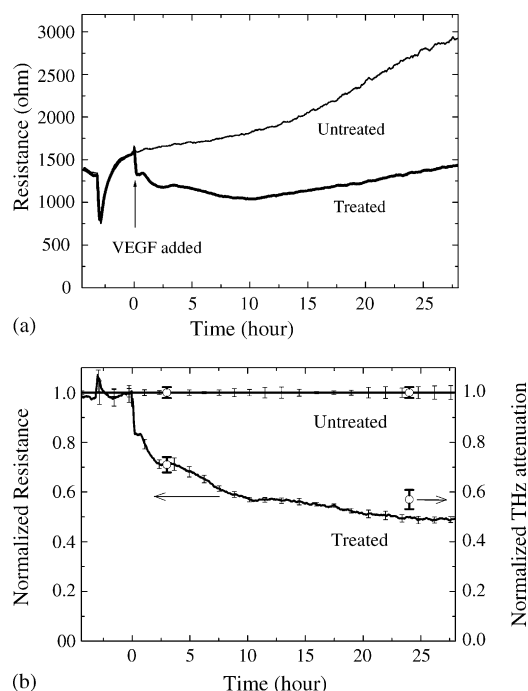


Fig. 4. (a) ECIS data vs. time for untreated and VEGF-treated BLMVEC. Time was set as 0 when VEGF was added to treat the sample. (b) A comparison between the ECIS and THz-DTDS results. The resistance and THz attenuation are normalized to those of the untreated samples. The solid curves are ECIS data and the open circles are THz-DTDS data, with error bars indicated, respectively.

the differences in THz-DTDS peaks. Because the plasma membrane of cells is a very poor conductor, electrical current flows primarily through the intercellular spaces, such that transendothelial resistance increases as cells grow more confluent and the intercellular spaces become smaller. Once cells reach 100% confluence, the resistance is almost entirely dependent upon the structural integrity of tight junctions formed between neighboring cells. When this resistance is plotted against time, as shown in Fig. 4(a), we can detect even small changes in tight junction integrity, indicated by drops in resistance. Prior to the addition of VEGF, the AC resistance of the two BLMVEC monolayer samples were approximately equal. However, the resistance decreased immediately after addition of VEGF, then slowly “rebounded” as a result of the morphology changes affected by VEGF.

The resistance difference between treated and untreated monolayers increased from 29% after 3 h to 50% after 1 day of VEGF exposure, which is remarkably close to the THz-DTDS results in Fig. 2(a). Fig. 4(b) presents a comparison between the normalized AC resistance (ECIS) and THz-DTDS attenuation data over time, and they agree very well. The error bars in Fig. 4(b) represent the standard deviations of three independent measurements for three groups of cell samples prepared under the same conditions. The standard deviations were 0.4–5% for ECIS data and 2–4% for THz-DTDS data. The ECIS data confirm the morphology change of the cells detected with THz-DTDS. Further analysis of the ECIS and THz-DTDS results requires additional modeling of the ECIS output (Giaever and Keese, 1991) and is not covered here.

3.3. Advantages and challenges of THz-DTDS

THz-DTDS offers several advantages over existing techniques such as ECIS for sensing subtle changes in cultured cells. First, ECIS cannot reliably measure subtle variations in cell thickness or rearrangements in cell architecture (reflected by changes in dielectric property) that do not affect inter-cell spacing, but these properties are readily detectable with THz-DTDS. Second, THz photons have energies on the meV scale, which is 1/1000 of the photon energy of visible light. Therefore, THz waves are completely non-invasive for *living* cells. Third, ECIS requires plating cells on a customized substrate containing gold film electrodes, whereas THz-DTDS can measure cell layers cultured on standard polystyrene or glass substrates. Finally, THz-DTDS extends the electromagnetic spectral measurement of cells to the THz range, a relatively unexplored space. THz-DTDS is promising to provide THz spectral information unavailable through other conventional methods like optical phase contrast microscope and ECIS.

Some challenges remain to be solved for THz-DTDS to become an applicable cell sensing technology. First, in transmission-based measurements, the cell samples must be extracted from the culturing medium to avoid the tremendous THz absorption of bulk water. Reflection-based THz spectroscopy may provide a solution to avoid this problem. Second, powerful THz sources and efficient THz detection methods need further improvements for more sensitive and real-time measurements. Finally, it is still challenging to employ the current THz-DTDS as an affordable biosensor, due to its cumbersome size and the high expense of femtosecond lasers. However, with the development of THz technology, THz spectroscopy integrated in chip with cell culturing may conceivably be implemented as a biosensor.

4. Conclusion

In this work, we have demonstrated the use of THz-DTDS for quantitatively measuring minute changes in cell monolayers. THz-DTDS has a particular appeal as a complementary technique, when used in conjunction with an optical microscope or ECIS, to measure properties of live cells, including cell growth, cell volume and morphology changes over time. Currently, to avoid bulk water absorption, cell samples need to be extracted from the medium for free-space measurements. Our future studies will concentrate on in situ reflection measurements of cultured cell monolayers within a medium.

Acknowledgements

This work was partly supported by the U.S. National Science Foundation. We would also like to thank Dr. Guo Chen, Mr. Chunzhi Dong, Dr. Charles R. Keese and Dr. Ivar Giaever for technical assistance with ECIS.

References

- Born, M., Wolf, E., 1970. Principles of Optics, fourth ed. Pergamon Press, New York.

- Fischer, B.M., Walther, M., Jepsen, P.U., 2002. *Phys. Med. Biol.* 47, 3807–3814.
- Giaever, I., Keese, C., 1991. *Proc. Natl. Acad. Sci. U.S.A.* 88, 7896–7900.
- Giaever, I., Keese, C., 1993. *Nature* 366, 591–592.
- Jiang, Z., Li, M., Zhang, X.-C., 2000. *Appl. Phys. Lett.* 76, 3221–3223.
- Lisin, R., Ginzburg, B.Z., Schlesinger, M., Feldman, Y., 1996. *Biochim. Biophys. Acta* 1280, 34–40.
- Markelz, A., Whitmire, S., Hillebrecht, J., Birge, R., 2002. *Phys. Med. Biol.* 47, 3797–3805.
- Menikh, A., Mickan, S.P., Liu, H., MacColl, R., Zhang, X.-C., 2004. *Biosens. Bioelectron.* 20, 658–662.
- Mickan, S.P., Menikh, A., Liu, H., Mannella, C., MacColl, R., Abbott, D., Munch, J., Zhang, X.-C., 2002. *Phys. Med. Biol.* 47, 3789–3795.
- Nagel, M., Bolivar, P.H., Brucherseifer, M., Kurz, H., Bosserhoff, A., Bu, R., 2002. *Appl. Phys. Lett.* 80, 154–156.
- Ronne, C., Thrane, L., Astrand, P.O., Wallqvist, A., Mikkelsen, K.V., Keiding, S.R., 1997. *J. Chem. Phys.* 107, 5319–5331.
- Woodward, R.M., Cole, B.E., Wallace, V.P., Pye, R.J., Arnone, D.D., Linfield, E.H., Pepper, M., 2002. *Phys. Med. Biol.* 47, 3853–3863.
- Wu, Q., Litz, M., Zhang, X.-C., 1996. *Appl. Phys. Lett.* 68, 2924–2926.
- Yamaguchi, M., Miyamaru, F., Yamamoto, K., Tani, M., Hangyo, M., 2003. *Technical Digest of Conference on Lasers and Electro-Optics/Quantum Electronics & Lasers Science Conference 2003*, Baltimore, MD, Paper no. CThPDD10.